AN ANALYSIS OF A SLOTTED WAVEGUIDE, FREQUENCY SCANNED, ANTENNA NEAR CUTOFF

M. R. Weiss

Mitre Corporation

Prepared for:

Electronic Systems Division

November 1974

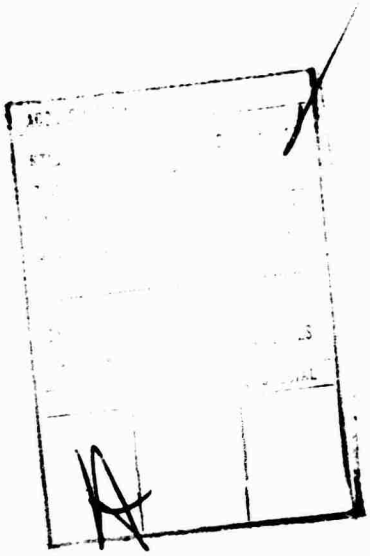

When U.S. Government drawings, specifications, or other data are used for any purpose other than a definitely related government procurement operation, the government thereby incurs no responsibility nor any obligation whatsoever; and the fact that the government may have formulated, furnished, or in any way supplied the said drawings, specifications, or other data is not to be regarded by implication or otherwise, as in any manner licensing the holder or any other person or corporation, or conveying any rights or permission to manufacture, use, or sell any patented invention that may in any way be related thereto.

Do not return this copy. Retain or destroy.

REVIEW AND APPROVAL

"This technical report has been reviewed and is approved for publication."

John F Donegan

JOHN F. DONEGAN
Project Engineer

JOSEPH L. MASI, Colonel, USAF
Director, Technology
Deputy for Planning, Technology
and Requirements

SECURITY CLASSIFICATION OF THIS PAGE (When Data Entered)

AD/A003 411

REPORT DOCUMENTATION PAGE

READ INSTRUCTIONS BEFORE COMPLETING FORM

1. REPORT NUMBER: ESD-TR-74-197	2. GOVT ACCESSION NO.
3. RECIPIENT'S CATALOG NUMBER	
4. TITLE (and Subtitle): An Analysis of a Slotted Waveguide, Frequency Scanned, Antenna Near Cutoff	5. TYPE OF REPORT & PERIOD COVERED
6. PERFORMING ORG. REPORT NUMBER: MTR-2841	
7. AUTHOR(s): M. R. Weiss	8. CONTRACT OR GRANT NUMBER(s): F19628-71-C-0002
9. PERFORMING ORGANIZATION NAME AND ADDRESS: The MITRE Corporation, Box 208, Bedford, Mass. 01730	10. PROGRAM ELEMENT, PROJECT, TASK AREA & WORK UNIT NUMBERS: Project No. 7080
11. CONTROLLING OFFICE NAME AND ADDRESS: Deputy for Planning, Technology and Requirement, Electronics System Division, AFSC, L. G. Hanscom Field, Bedford, Mass. 01730	12. REPORT DATE: November 1974
	13. NUMBER OF PAGES: ~~51~~ 53
14. MONITORING AGENCY NAME & ADDRESS(if different from Controlling Office)	15. SECURITY CLASS. (of this report): Unclassified
	15a. DECLASSIFICATION/DOWNGRADING SCHEDULE

16. DISTRIBUTION STATEMENT (of this Report)

Approved for public release; distribution unlimited.

17. DISTRIBUTION STATEMENT (of the abstract entered in Block 20, if different from Report)

18. SUPPLEMENTARY NOTES

19. KEY WORDS (Continue on reverse side if necessary and identify by block number)

Frequency Scan Antenna
Limited Scan Antenna

20. ABSTRACT (Continue on reverse side if necessary and identify by block number)

Two major concerns in the designs of X-Band precision approach radars are their cost and their ability to detect and track aircraft in heavy rain clutter. The objective of this investigation was to study a particular limited scan, linearly polarized antenna which could be used in conjunction with a digital filter for the suppression of clutter and thereby provide a low cost system concept. This antenna uses the inherent dispersion of slotted waveguide near cutoff for frequency scan in elevation. However,

DD FORM 1 JAN 73 1473 EDITION OF 1 NOV 65 IS OBSOLETE

SECURITY CLASSIFICATION OF THIS PAGE (When Data Entered)

such antennas are sensitive to waveguide dimensional errors. This report presents an analysis of the effect of such errors on the formation of the frequency scanned beam. Basic design equations are developed for a narrow scan angle application. The effect of statistical errors is analyzed and average radiation patterns are presented which indicate the degree of degradation.

TABLE OF CONTENTS

LIST OF ILLUSTRATIONS

SECTION I

INTRODUCTION

The primary function of precision approach radars is the detection and tracking of landing aircraft during final approach, oftentimes in the presence of heavy rainfall clutter. Because the operation of such radars has been restricted to X-Band and because the radar cross section of rain is an increasing function of frequency, techniques for discrimination of aircraft from rain clutter are of major concern to the system design process. Available discrimination techniques are (1) the use of circular polarization, (2) the use of high range resolution, and (3) the use of Doppler resolution or MTI. For example, the AN/TPN-19 PAR uses a combination of all three, each contributing toward the whole. However, this design approach has proved costly. Currently, the AN/GPN-XX PAR program is considering approaches of lower cost potential.

In order to provide an enlarged technical data base applicable to the AN/GPN-XX program, Project 7080 entitled Aircraft Detection in Rain was conducted in Fiscal Year 1974 for the Electronic Systems Division, USAF, by the MITRE Corporation. This project embraced three specific tasks: (1) the experimental measurement of the depolarization of circular polarization by rain at X-Band, (2) the investigation of a linearly polarized, low cost, electronically scanned antenna, and (3) the application of digital filtering techniques to the discrimination

of rain clutter through Doppler resolution of target and clutter. As a result of a review of this project by the Rome Air Development Center in its early stages, the application of effort applied to the depolarization measurements was emphasized and that applied to the antenna and digital filtering tasks were diminished.

This report presents the results of the low cost antenna study. The results of the study of circular polarization degradation are given in Reference 1 and those of the digital filtering study are given in Reference 2. The principal conclusions of this study are that a low cost limited scan antenna of the linearly polarized, frequency-phase scan type using slotted waveguide near cut-off appears feasible and that its use in conjunction with the digital filtering techniques of Reference 2 could possess significant potential for a low cost system design. The degradation data of Reference 1 on the other hand should be useful to system design concepts which utilize circular polarization inasmuch as very little data of this kind is available.

The low cost antenna study of this report begins with a brief description of the AN/TPN-19 antenna design and then considers alternatives having limited angular scan capabilities. Among these, the concept of frequency scan in elevation using the inherent dispersion of slotted waveguide near cut-off is analyzed with respect to the effect of waveguide dimensional errors on the formation of the frequency scanned beam. Such an antenna could utilize phase shifters for azimuth scan.

The AN/TPN-19 is an electronically scanned X-Band, narrow beam, limited scan, radar system designed for application as an aircraft precision approach radar (PAR). The narrow beamwidth requirement (1.4° in azimuth and 0.75° in elevation) would normally result in a large antenna, with many elements and phase shifters, which in general would drive the cost unacceptably high. The limited scan requirement, on the other hand, does allow antenna approaches which can result in cost saving features.

The present AN/TPN-19 antenna design[3] is made up of an array-reflector combination. The narrow beamwidth is accomplished by a large effective aperture paraboloidal reflector steered by a much smaller planar phased array. The basic antenna geometry is shown in Figure 1. The feed horn, shown at point S, radiates energy toward a reflect array lens centered at point L. This lens consists of a planar array of pick up horns terminated in an electronic phase shifter. This intermediate lens reradiates the energy with proper phasing toward the parabaloidal reflector. The phasing at the surface of the paraboiloid can be produced such that a pencil beam is generated in a predetermined direction within the required scan volume.

While theoretically sound, this approach has resulted in a relatively high cost design. Several alternatives have, therefore, been under investigation during the past year in the limited scan array area.

The large majority of work in this area is associated, either directly, or via subcontract with the Air Force Cambridge Research Laboratories (AFCRL). In one phase of this work an attempt to improve the AN/TPN-19 antenna concept has been under study of AFCRL. This work being carried out by A. Schell is an investigation aimed at a more optimum choice of the AN/TPN-19 antenna parameters. To this end a systematic study of reflector shape, array shape and the general antenna geometry has been done. Partial results were presented at the 1973 PGAP Antenna Symposium[4].

In another study being carried out at AFCRL, R. Mailloux has been considering a planar phased array using large (4λ), widely spaced elements. The principal problem in this design is suppression of the resulting grating lobes. The generation of odd modes has been successful in canceling the dominant E-plane grating lobe. The results of this work was reported at the 1973 PGAP[5] as well as in Reference 6.

An AFCRL subcontract with Raytheon has resulted in a dual lens antenna concept. This design consists of three antenna components: an aperture lens, a focal field matching lens and a phased array feed (see Figure 2). This results of an experimental program using this design is given in Reference 7.

The study here at MITRE and the subject of this paper deals with the application of a frequency scanned array, in the elevation plane, using slotted waveguide. The unique feature is that high scan sensitivity is achieved by operating near the dominant mode cutoff and,

therefore, making use of the highly non-linear waveguide propagation characteristics in this region.

In the sections which follow the general array relationships are developed. Scan sensitivity and waveguide losses are examined. The sensitivity of the design with respect to waveguide parameters increases the significance of design tolerances. As a result, the emphasis of the remainder of the paper is related to a theoretical analysis on the effects of random errors.

In particular, the effect of errors on the antenna radiation pattern, beamwidth and pointing accuracy is presented. As a supplement to this analysis a discussion of error sources is given.

SECTION II

FREQUENCY SCAN ANTENNA

The antenna configuration under investigation is a section of rectangular waveguide, terminated at one end by a matched absorber and fed by a matched, frequency swept, generator. Radiating slots are cut in the narrow wall of the waveguide and their coupling adjusted to provide a predetermined amplitude distribution over the slots. The basic gredients of this configuration are presented in Figure 3.

In Figure 3 are shown N + 1 slots separated by a distance d, for which the radiation pattern is given by the expression:

$$E(\theta,\phi) = \sum_{m=-N/2}^{N/2} A_m(\theta,\phi)\, I_m e^{-j\alpha_m} \cdot e^{jmkd\sin\theta\cos\varphi} \qquad (1)$$

where,

$A_m(\theta,\phi)$ = element pattern

$I_m e^{-j\alpha_m}$ = complex amplitude at the m^{th} element

$k = \frac{2\pi}{\lambda}$ = free space wave number

We assume that the element pattern (i.e., slot radiation pattern) is independent of m and set $A_m(\theta,\phi) = A_o(\theta,\phi)$. Furthermore, the element phase is determined by, k_g, the wavenumber in the guide and can be expressed as

$$\alpha_m = mk_g d. \qquad (2)$$

Defining the array factor as $f(\theta,\phi)$ we can express Equation (1) in the form:

$$f(\theta,\phi) = \sum_{m=-N/2}^{N/2} I_m e^{-jmk_g d} \cdot e^{jmkd\sin\theta\cos\phi} \tag{3}$$

From Equation (3), the pointing angle (direction of the main beam) is given by the principal maximum in the radiation pattern. This occurs when each term of the sum adds in phase, i.e., when

$$m\,kd\sin\theta\cos\phi - mk_g d = \pm 2N\pi \tag{4}$$

where N = 0, 1, 2 . . .

We restrict our attention to the lowest order beam maximum (N=0) and the ϕ=0 plane which reduces equation (4) to:

$$\sin\theta = \frac{k_g}{k} \tag{5}$$

The guide wave number, $k_g = 2\pi/\lambda_g$, refers to the dominant mode in rectangular waveguide and is given by

$$k_g = k\left[1 - (\lambda/\lambda_c)^2\right]^{1/2} \tag{6}$$

For the rectangular guide being considered the cutoff wavelength, λ_c is twice the large cross section dimension of the waveguide ("a" in Figure 3). With this substitution equation 5 and 6 provides the basic scan equation.

$$\theta = \cos^{-1}\left(\frac{\lambda}{2a}\right) \qquad 0 \leq \theta \leq \pi/2 \tag{7}$$

From equation (7) we see the inherent utility of operating near cutoff for narrow scan application. Away from cutoff, where $\lambda/2a$ is $<< 1$, equation (7) shows that the scan angle changes linearly with λ according to the formula:

$$\theta \approx \pi/2 - \lambda/2a \tag{8}$$

On the other hand near cutoff, $\lambda/2a \approx 1$, equation (7) takes on the non-linear form:

$$\theta \approx [1 - (\lambda/2a)^2]^{1/2} \tag{9}$$

The highly non-linear properties of the scanning equation near cutoff is better demonstrated by considering the sensitivity relation $d\theta/d\lambda$ given by Equation (10).

$$\frac{d\theta}{d\lambda} = \frac{1}{2a[1 - (\lambda/2a)^2]^{1/2}} \tag{10}$$

We note that as we approach cutoff this derivative becomes infinite.

Figure 4 presents the basic scan parameters. It is assumed that the radiation pattern is scanned symmetrically by an amount α about

a central angle θ_o. With reference to array broadside, the beam is, therefore, scanned between angles θ_1 and θ_2 (corresponding to $\theta_o \pm \alpha$) at frequencies associated with the wavelengths λ_1 and λ_2. Utilizing equation (7) for these two wavelengths it is seen that:

$$\begin{aligned} \cos(\theta_o + \alpha) &= \lambda_2/2a \\ \cos(\theta_o - \alpha) &= \lambda_1/2a \end{aligned} \qquad \lambda_1 > \lambda_2 \qquad (11)$$

When the relationships in Equation (11) are combined we get the result:

$$\tan\theta_o = \frac{\lambda_2 - \lambda_1}{\lambda_2 + \lambda_1} \operatorname{ctn}\alpha \qquad (12)$$

In general it is desirable to scan near array broadside (θ_o near zero) so that most of the full aperture area is utilized in forming the narrowest beam for all scan angles. It is seen from Equation (12) that a small central angle, θ_o, corresponds to a narrow operating bandwidth. This in turn produces a large scan sensitivity, $d\theta/d\lambda$, which results in the desired scanning range $(\theta_1 - \theta_2) = 2\alpha$.

These results are best indicated by expressing Equation (12) in terms of required bandwidth (BW). If we define f_c, as the cutoff frequency of the waveguide under consideration we get the transcendatal equation

$$\frac{\cos\theta_1 - \cos\theta_2}{\cos\theta_1 \quad \cos\theta_2} - \frac{BW}{f_c} = 0 \quad . \qquad (13)$$

Equation (13) is presented graphically in Figure 5. We see in this figure that in general, restricting the bandwidth results in a frequency operating range nearer to cutoff; how close to cutoff is determined by the extent of the angular scan required. A typical case of interest can be evaluated for standard X-band waveguide with cutoff frequency $f_c = 6.55678 \times 10^9$ Hz ($\lambda_c = 4.572$cm). If we desire $\pm$ 4° of scan with a 200 MHz bandwidth we find

$$\text{Bandwidth}/f_c = 3.05 \times 10^{-2}$$

and

$$\lambda_1/\lambda_c = 0.982$$

with the array scanning from 9° to 17°.

The same angular scan of $\pm$ 4° but with a 400 MHz bandwidth results in

$$BW/f_c = 6.10 \times 10^{-2}$$

$$\lambda_1/\lambda_2 = 0.910$$

and

$$\theta_2 - \theta_1 \Rightarrow 25° - 33°$$

While differences in results for the two assumed bandwidths are not startling the question of how close to cutoff we operate has subtle implications (we note that doubling the bandwidth has changed the ratio λ/λ_c from 0.982 to 0.910).

One factor to consider is ohmic losses in the waveguide. Standard formulas for dominant mode propagation give this[6] as

$$L \text{ (dB/meter)} = 8.686 \frac{R_s}{b\sqrt{\mu_0/\epsilon_0}\sqrt{1 - (\lambda/\lambda_c)^2}} \left[1 + \frac{2b}{a} \left(\frac{\lambda}{\lambda c}\right)^2\right] \quad (14)$$

In Equation (14) b and a are the narrow and broadface wall dimensions, R_s is the surface resistance[7] of the waveguide material with $\sqrt{\mu_o/\epsilon_o}$ being the impedance of free space.

Figure 6 shows results for standard X-band waveguide for two conducting materials (for this waveguide the ratio a/b = 2.25). In general, we see that ohmic losses are small (for a moderate length array). However, beyond the "knee" region losses increase rapidly as we approach the cutoff wavelength. For silver the knee occurs at $\lambda/\lambda c \simeq .99$, while for brass this ratio is $\lambda/\lambda c \simeq .98$. It would appear, for most materials, that operating below $\lambda/\lambda c$ of 0.99 is desirable.

Another important consideration is the sensitivity of scan angle with errors in the prescribed value of cutoff wavelength. In general, the waveguide broadface dimension, which determines the cutoff wavelength, is toleranced to several thousandths of an inch. While this tolerance is adequate when operating away from cutoff the situation is

not as clear when operating near cutoff. It is anticipated that slight changes of the broadface, from its design value, can result in large errors in scan angle when operating very near cutoff. Using Equation (7), this effect can be analysed by considering the sensitivity equation:

$$\frac{d\theta}{da} = \frac{1}{a} \quad \frac{\lambda/\lambda c}{\sqrt{1-\left(\lambda/\lambda c\right)^2}} \qquad (15)$$

This result is plotted in Figure 7. Once again we see highly non-linear effects occurring for $\lambda/\lambda c \gtrsim 0.99$ where $\frac{d\theta}{da} \simeq 7$ radians. Expressed in terms of the waveguide we have been considering (a=2.28cm)

$$\frac{d\theta}{da} = 3.1 \text{ radians/cm}$$

or about a 0.5° error for a 10^{-3} inch error in broadface dimension. This result indicates that tolerance in the broadface waveguide dimension and, therefore, the specification of cutoff wavelength is likely to have a significant effect when operating near cutoff.

What is also raised by this result is the general question of the effect of errors and tolerances on the ultimate performance of the frequency scan antenna near cutoff. While it is true that many of the errors can be considered as fixed biases which can be "tuned out", there does exist a class of errors which are statistical in nature which degrade the overall antenna performance. It is this class which we explore in the following Section.

SECTION III

STATISTICAL ANALYSIS

Our analysis of the frequency scan antenna in the previous Section has shown that the antenna array pattern is expressible in the form

$$f(\theta,\phi) = \sum_{m=-N/2}^{N/2} I_m e^{-j\alpha_m} \cdot e^{jmkd\sin\theta\cos\phi} \qquad (16)$$

The quantity, α_m, is the element phase and is given by $\alpha_m = mk_g d$ for the case of constant element spacing d and guide wavenumber k_g.

The choice of element amplitude and phase (I_m and α_m respectively) is governed by the antenna sidelobe requirement (amplitude taper) and steering requirements of the antenna. In the course of constructing the antenna, however, design criteria cannot always be exactly met. These imperfections in turn result in radiation pattern characteristics different than originally desired.

The analysis of the effect of errors is best handled statistically. That is, we consider a large number of identically designed antennas, constructed to within given tolerances. A statistical ensemble results which then provides information on the average and variance of the resulting ensemble patterns. In general, if tolerances are held tightly the variance will be small and the ensemble of antennas will produce radiation patterns which are all very close to the desired one.

A. Average Radiation Pattern

A statistical analysis of the antenna radiation pattern* proceeds by assuming that particular quantities in the sum of equation (16) are random variables. The antenna pattern itself then becomes a function of random variables. We will assume a large number of such antennas, each described by equation (16), but with radiation patterns which vary randomly from each other. The average antenna pattern will then become the antenna pattern resulting from the average over this ensemble.

For convenience, we rewrite Equation (16) in an integral form and introduce the random error quantities as indicated.

$$f(\theta,\phi) = \int_{-L/2}^{L/2} A_o(x) e^{B(x) + j\phi(x)} \, e^{-j\int_{-L/2}^{x} k_g(x')dx'} e^{jkx\sin\theta\cos\phi} \, dx \qquad (17)$$

Equation (17) has been written for a continuous aperture but with the following assumption applying for the discrete case:

$$A_o(x) \equiv \sum_{m=-N/2}^{N/2} I_m \delta(x-md) \qquad N \equiv L/2d$$

Also in Equation (17) $B(x)$, $\phi(x)$ and $k_g(x)$ are assumed to be random functions which describe the errors in the element amplitude, phase and waveguide number respectively. The amplitude error is defined such that $A(x) \equiv A_o(x)\, e^{B(x)}$ where $A_o(x)$ is the no error amplitude.

* The analysis which follows is based upon the methods and assumptions used in Reference 8 where closed form results were achieved for a uniformally illuminated continuous linear array.

In order to proceed, the various error terms must first be modeled by suitable probability density functions (pdf's). The exact nature of the pdf describing these variables is of course related to the many sources of errors which make up the antenna and in general are unknown. We will set aside an analysis of error sources and assume that $B(x)$, $\phi(x)$, and $k_g(x)$ are normally distributed random functions. While the approximations of this assumption would appear to be difficult to substantiate the fact that a large number of independent random error sources contribute to the behavior of these random functions would suggest an application of the central limit theorem[9].

In any event we proceed with the assumption of normal distributions and define the means and variances thusly

$$\overline{B(x)} = B_o$$

$$\overline{\phi(x)} = 0$$

$$\overline{k_g}(x) = k_{g_o} \quad \text{(no error wave number)} \tag{18}$$

$$\overline{[B(x) - B_o]^2} \equiv \sigma_B^2$$

$$\overline{\phi^2}(x) \equiv \sigma_\phi$$

$$\overline{\Delta k_g^{\,2}} = \overline{(k_g(x) - k_{g_o})^2} = \sigma_{k_g}^2$$

We will require the correlation coefficients which are defined the usual way by:

$$r_B(x, x_1) \equiv \frac{\overline{[B(x) - B_o]\,[B(x_1) - B_o]}}{\sigma_B^2}$$

$$r_\phi(x, x_1) = \frac{\overline{\phi(x)\,\phi(x_1)}}{\sigma_\phi^2} \qquad (19)$$

$$r_{k_g}(x, x_1) = \frac{\overline{\Delta k_g(x)\,\Delta k_g(x_1)}}{\sigma_{k_g}^2}$$

and the cross-correlation coefficients

$$r_{B\phi}(x, x_1) = \frac{\overline{[B(x) - B_o]\,\phi(x_1)}}{\sigma_B \sigma_\phi}$$

$$r_{k_g B}(x, x_1) = r_{k_g \phi}(x, x_1) = 0$$

(a reasonable assumption which furthermore simplifies the results which follow)

In all of the above definitions it is understood that averaging is done over the ensemble of antennas for fixed argument "x". In general, therefore, the means and variances will be functions of "x".

The farfield radiation pattern is proportional to the absolute magnitude of equation (17) and is given by

$$\left|f(\theta,\phi)\right|^2 = \iint_{-L/2}^{L/2} A_o(x)A_o(x_1)\, e^{B(x) + B(x_1) + j\,[\phi(x) - \phi(x_1)]} \tag{20}$$

$$x\, e^{j\int_x^{x_1} \Delta k_g(x')dx'} \cdot e^{-j(x-x_1)\,\psi(\theta,\phi)}\, dxdx_1$$

where $\psi(\theta,\phi) \equiv k_{g_o} - k\sin\theta\cos\phi$

For now, what we are really interested in is the average antenna pattern $\overline{\left|f(\theta,\phi)\right|^2}$. Two factors in the integrand must be considered for this averaging; they are:

$$\overline{e^{B(x) + B(x_1) + j[\phi(x) - \phi(x_1)]}} \qquad \text{(a)} \tag{21}$$

and

$$\overline{e^{j\int_x^{x_1} \Delta k_g(x')dx'}} \qquad \text{(b)}$$

A general formula for normally distributed variables which can be used to reduce Equation 21(a) tells us that:

$$\overline{e^{j[a_1x_1 + a_2x_2 + a_3x_3 + a_4x_4]}} = e^{j\sum_{k=1}^{4} \overline{x_k}a_k - \frac{1}{2}\sum_{i=1}^{4}\sum_{k=1}^{4} \sigma_i\sigma_k r_{ik}a_i a_k} \quad (22)$$

Therefore, the average pattern takes on the form:

$$\left|f(\theta,\phi)\right|^2 = \iint_{-L/2}^{L/2} A_o(x)A_o^*(x_1)\, e^{2B_o} \cdot e^{-\frac{1}{2}\Delta(x,\, x_1)} \cdot e^{j\int_{x}^{x_1} \Delta kg(x')dx'} \times e^{-j(x-x_1)\,\psi(\theta,\phi)}\, dx\,dx_1 \quad (23)$$

with $\Delta(x, x_1) = 2\sigma_\phi^2 - 2\sigma_B^2 - 2\sigma_B^2\, r_B(x,x_1) - 2\sigma_\phi^2\, r_\phi(x,x_1)$

We see now that the assumption of vanishing cross-correlation coefficients, $r_{k_g B}$, $r_{k_g \phi}$ has allowed us to explore the averages in 21(a) and 21(b) separately. We also note that the result in equation (23) is independent of the cross-correlation term $r_{B\phi}$ which we have not made any assumptions about.

In the context of the statistical modelling employed our solution is still general. At this point, however, we can relax some constraints. The factor $\Delta(x, x_1)$, in general, contains variances which depend on "x" as well as the correlation coefficients $r_B(x, x_1)$ and $r_\phi(x, x_1)$.

We expect, however, that the element (a slot) amplitude and phase errors are sufficiently random so that we may set the variances to a constant and, therefore, remove them from the integral.

$$\overline{|f(\theta,\phi)|^2} = e^{2B_o} + \sigma_B^2 - \sigma_\phi^2 \iint_{-L/2}^{L/2} A_o(x)A_o^*(x_1) + e^{\sigma_B^2 r_B(x,x_1) + \sigma_\phi^2 r_\phi(x,x_1)} \cdot \overline{e^{j\int_x^{x_1}\Delta k_g(x')dx'}} \cdot e^{-j(x-x_1)\psi(\theta,\phi)}dxdx_1 \tag{24}$$

The averaging of the remaining exponential (equation 21(b) is once again simplified for the case of a normally distributed variable. We have

$$\overline{e^{j\int_x^{x_1}\Delta kg(x')dx'}} = e^{-\frac{1}{2}\overline{\left[\int_x^{x_1}\Delta kg(x')dx'\right]^2}} \tag{25}$$

with the additional result

$$\overline{\left[\int_x^{x_1}\Delta kg(x')dx'\right]^2} = \iint_x^{x_1}\overline{\Delta kg(x')\Delta kg(x'')\,dx'dx''} = \sigma_{k_g}^2\iint_x^{x_1} r_{k_g}(x',x'')dx'dx'' \tag{26}$$

Substituting this result into Equation (24) provides:

$$\overline{|f(\theta,\phi)|^2} = e^{2B_o} + \sigma_B^2 - \sigma_\phi^2 \iint_{-L/2}^{L/2} A_o(x)A^*(x_1)\, e^{\sigma_B^2 r_B(x,x_1) + \sigma_\phi^2 r_\phi(x,x_1)} \cdot e^{-\frac{1}{2}\sigma_{k_g}^2 \iint_x^{x_1} r_{k_g}(x',x'')dx'dx''} \cdot e^{-j(x-x_1)\psi(\theta,\phi)}dxdx_1 \tag{27}$$

Equation (27) reveals several interesting features. We note first that distortion of the mean radiation pattern occurs in the same way for either amplitude or phase errors since σ_B^2, r_B and σ_ϕ^2, r_ϕ are involved in the integral in the identical form. The factor $\exp\left|2B_o + \sigma_B^2 - \sigma_\phi^2\right|$ behaves as a scaling factor. Another point we have already mentioned is the fact that our result is independent of any correlation between amplitude and phase errors but only depends on the correlation coefficients $r_B(x, x_1)$ and $r_\phi(x, x_1)$. If we now in fact consider results when only weak correlation exists* the amplitude and phase errors appear in the integral only as a multiplicative factor.

This result points out examples of two general classes of statistical errors. These classes are referred to as "local" and "nonlocal" errors. Local errors, while having an overall effect on the radiation

*In terms of a correlation length, ρ, this means that $\rho >> L$.

pattern, is an error which influences the characteristics of a single element without affecting (at least to first order) the characteristics of other elements. Generally speaking the radiation pattern effects of local errors is small compared to the effects of non-local errors. The non-local error is cumulative and, while its source can be local, has effects which propagate along the antenna. It is this class which is more appropriate to the travelling wave type antenna we are considering.

In Equation (27) the local errors (in the uncorrelated case) manifest themselves as a factor appearing outside the integral. The non-local error which in this example is the randomness of k_g, is a function of the positions "x" and "x_1" along the antenna. We note for example, that even for the uncorrelated case the error due to randomness in wavenumber is proportional to

$$e^{-\frac{1}{2}\sigma_{k_g}^2 (x_1 - x)^2} \tag{28}$$

the cumulative nature indicated by the $(x_1 - x)^2$ factor.

In the numerical results to follow we will drop the contribution of local amplitude and phase errors and devote our attention to effects of guide wavenumber variation. What, therefore, remains from Equation (26) is a reduction of the integral:

$$\iint_{x}^{x_1} r_{k_g}(x', x'')dx'dx'' \tag{29}$$

With very little basis for choosing the form of the correlation coefficient $r_{k_g}(x', x'')$ our selection is somewhat arbitrary. In general, however, we expect a form which falls off with increasing $|x' - x''|$. For simplicity we choose the single parameter form:

$$r_{k_g}(x', x'') = e^{-|x' - x''|/\rho} \tag{30}$$

where $\rho \equiv$ correlation distance.

Other choices are of course possible, for example, the normal form

$$r_{k_g}(x', x'') = e^{-(x' - x'')^2/\rho^2}$$

however, in the final analysis, numerical results do not change appreciably with this choice. In any event, Equation (30) does produce a tractable result. From Equation (29) and (30) we get

$$\int_{x}^{x_1} e^{-|x' - x''|/\rho}\, dx'dx'' = 2\rho^2 \left[\frac{|x_1 - x|}{\rho} + e^{-|x_1 - x|/\rho} - 1\right] \tag{31}$$

Which gives us the result:

$$\overline{|f(\theta,\phi)|^2} = \int_{-L/2}^{L/2} A_o(x) A_o^*(x_1)\, e^{-\rho^2\sigma_{k_g}^2} \left[\frac{|x_1 - x|}{\rho} + e^{-|x_1 - x|/\rho} - 1\right] \cdot e^{-j(x - x_1)\psi(\theta,\phi)}\, dx\, dx_1 \tag{32}$$

We can if we wish now reformulate Equation (32) for the discrete aperture case which yields:*

$$\overline{|f(\theta,\phi)|^2} = \sum_{m=-N/2}^{N/2}\sum A_n A_m^* \exp\left|-\rho^2\sigma^2\left[\frac{|m-n|d}{\rho} + e^{-|m-n|d/\rho} - 1\right]\right| e^{-j\psi(m-n)d} \tag{33}$$

Equation (33) assumes N + 1 elements with spacing d. If the element strengths are symmetric i.e., $A_m = A_{-m}$ Equation (33) assumes the form:

$$\overline{|f(\theta,\phi)|^2} = 2\mathrm{Re}\left\{\sum_{m=-N/L}^{N/L}\sum_{n=-N/L}^{M} A_m A_n^* \exp\left\{-\rho^2\sigma^2\left[\frac{(m-n)d}{\rho} + e^{-(m-n)d/\rho} - 1\right]\right\} e^{-j\psi(m-n)d}\right\} - \sum_{-N/2}^{N/2}|A_m|^2 \tag{34}$$

with $\psi = \psi(\theta,\phi) = k_{g_o} - k\sin\theta\cos\phi$

Several numerical examples using Equation (34) have been calculated. For this purpose a travelling wave antenna consisting of 75 elements was chosen. An antenna length of $L/\lambda = 60$, was chosen to yield a half power beamwidth of 1° (this results in an element spacing $d/\lambda = 0.8$ which eliminates grating lobes for about 20° of scan). Various error variances and correlation lengths were included from $\sigma^2\lambda^2$ of .01 to

*To simplify notation $\sigma^2_{k_g}$ has been replaced by σ^2.

.003 and ρ/λ of .8 to ∞. The element amplitude themselves were chosen to produce a Taylor weighting of $\bar{n} = 4$ with 20dB sidelobes[10].

In Figure 8 for example, is the error free array pattern and results for various $\sigma^2\lambda^2$ values when the randomness of k_g is uncorrelated ($\rho/\lambda = \infty$). We note that an increase in the variance of k_g is at first accompanied by a filling of nulls with only slight effects in the main lobe peak. Larger values of $\sigma^2\lambda^2$ tend to produce an isotropic pattern. For a given value of $\sigma^2\lambda^2$, shown in Figure 9, we find for correlated errors ($\rho \to 0$) the pattern once again approaches the error free result.

B. Error Sources

In order to adequately interpret the results in Figures 9 and 10 we must first characterize the error magnitudes. Generally this is best done emperically, however, some insight is possible with the following analysis.

The principal source of non-local errors is in the statistical behavior of the wave number k_g. This is particularly true near cutoff, where slight departures of design parameters have large effects on the guide wave number and thereby degrading effects on the resulting radiation pattern. The guide wave number is given by

$$k_g = k\sqrt{1 - \left(\lambda/2a\right)^2} \tag{35}$$

where

$k = 2\pi/\lambda$ in free space.

From Equation (35) we see immediately that errors in k_g can result from inaccuracies in the broadface wall dimension "a". For purposes of calculation let us assume that this broadface wall dimension is a random variable uniformally distributed about its design value, a_o, such that in terms of a probability density function we have

$$p(a) = \frac{1}{2\Delta} \begin{cases} 1 & a_o - \Delta \leq a \leq a_o + \Delta \\ 0 & \text{otherwise} \end{cases} \tag{36}$$

For the case of standard waveguide, Δ, corresponds to the design tolerance of 0.003 inches. In practice errors in the "a" dimension can also result from a variety of sources (temperature, mechanical stress, etc.).

In any event given the pdf in Equation (36) one can by elementary methods calculate the mean and variance of the wave number k_g. We have that

$$\overline{k_g} = \int k_g(a)\ p(a)\ da$$

and

$$\sigma^2 \equiv (k_g - \overline{k_g})^2 = \int k_g^2(a)\ p(a)\ da - \overline{k_g^2} \tag{37}$$

The resulting integrals can be evaluated and yield:

$$\frac{\overline{k_g}}{k} = \frac{1}{4(\Delta/\lambda)} \left\{ (u^2 - 1)^{1/2} - \arccos 1/u \right\} \Bigg|_{u_-}^{u_+}$$

$$\frac{\overline{k_g^2}}{k^2} = \frac{1}{4(\Delta/\lambda)} \left\{ u + 1/u \right\} \Bigg|_{u_-}^{u_+} \qquad (38)$$

with $u_{\pm} = \frac{2a_o}{\lambda} \pm 2(\Delta/\lambda)$

The result of forming the variance, $\sigma^2\lambda^2$ is given in Figure 10. The ordinate is the spread in the broadside dimension, 2Δ, measured in terms of the free space wavelength λ.

An applicable numerical example would correspond to a design tolerance of $\pm$ 0.003" for standard X-band waveguide. For this example $\frac{2\Delta}{\lambda}$ is approximately $3x10^{-3}$ which results in $\sigma^2\lambda^2 \approx 10^{-3}$ for the ratios of λ/λ_c we are interested in. Figures 8 and 9 indicate that distortion of the antenna radiation pattern occurs for this range of error.

C. Beam Pointing Error

The average radiation patterns shown in Figures 8 and 9 indicate the effects of randomness in k_g on the main lobe and side lobe levels. These results, however, do not show the effect of random errors on beam pointing.

In order to analyze this we make a slight modification in our approach by considering results in the small error limit. We first rewrite Equation (17) in the form:

$$f(\psi) = \int_{-L/2}^{L/2} A(x)\, e^{-j\int_{-L/2}^{x} \Delta k_g(x')dx'}\, e^{-j\psi x}\, dx \tag{39}$$

We define Δk_g so that its mean value is zero

$$\Delta k_g \equiv k_g - \overline{k_g} \quad . \tag{40}$$

We further consider the azimuthal plane $\phi = 0$ so that

$$\psi \equiv \overline{k_g} - k\sin\theta \tag{41}$$

(k = free space wave number).

We note that in general, $\overline{k_g}$ does not correspond to the anticipated design value which we will denote by k_D.

In terms of the difference

$$\Delta k \equiv \overline{k_g} - k_D \tag{42}$$

Equation (41) becomes

$$\psi = k\left[\frac{\Delta k}{k} + \sin\theta_o - \sin\theta\right] \tag{43}$$

where, for the no-error case we make the definition

$$\sin\theta_o \equiv \frac{k_D}{k}$$

The angle θ_o represents the direction of the main beam when no errors exist. For the case where errors are present the direction of the principal maximum will actually be at $\theta=\theta_m$ (and $\psi = \psi_{max}$). Equation (43) when rewritten for this special direction becomes:

$$\sin\theta_o - \sin\theta_m = \frac{1}{k}(\psi_{max} - \Delta k) \tag{44}$$

If we now assume that $\Delta\theta \equiv \theta_o - \theta_m$ is small we achieve the results

$$\begin{aligned} \overline{\Delta\theta} &\simeq \frac{1}{k}(\overline{\psi_{max}} - \overline{\Delta k}) \\ \overline{\Delta\theta^2} &\simeq \frac{1}{k^2}(\overline{\psi_{max}^2} + \overline{\Delta k^2} - 2\overline{\Delta k}\,\overline{\psi}_{max}) \end{aligned} \tag{45}$$

An interpretation of Equation (45) depends on an evaluation of the statistical quantities $\overline{\psi}_{max}$ and $\overline{\psi_{max}^2}$ which we now proceed to develop.

Returning to Equation (39), we define the random phase in the integral as

$$\phi(x) \equiv \int_{-L/2}^{x} \Delta k_g(x')dx' \tag{46}$$

such that from Equation (40)

$$\overline{\phi(x)} = 0.$$

We assume that this phase error is small and, therefore, keep only the leading terms of the exponential in Equation (39) resulting in:

$$f(\psi) = \int_{-L/2}^{L/2} A(x)\, e^{-j\psi x}\, dx - j \int_{-L/2}^{L/2} A(x)\, \phi(x)\, e^{-j\psi x}\, dx + \frac{1}{2} \int_{-L/2}^{L/2} A(x)\, \phi^2(x)\, e^{-j\psi x}\, dx \tag{47}$$

The radiation pattern is proportional to

$$|f(\psi)|^2 \simeq \left[\int_{-L/2}^{L/2} A(x)\, e^{-j\psi x}\, dx\right]^2 - 2 \iint_{-L/2}^{L/2} A(x)A^*(x_1)\phi(x)\sin\psi(x - x_1)\, dxdx_1 - \iint_{-L/2}^{L/2} A(x)A^*(x_1)\, \phi^2(x)\, \cos\psi(x - x_1)\, dxdx_1 + \left[\int_{-L/2}^{L/2} A(x)\phi(x)\, \cos\psi x dx\right]^2 + \left[\int_{-L/2}^{L/2} A(x)\phi(x)\, \sin\psi x dx\right]^2 \tag{48}$$

Recognizing that for small $\phi(x)$ the principal maximum will not be far from $\psi = 0$ we approximate

$$\sin\psi x \to \psi x$$

$$\text{and} \quad \cos\psi x \to 1 - \frac{\psi^2 x^2}{2}$$

which to second order in ψ yields

$$\left|f(\psi)\right|^2 \simeq I_o^2 + \left[\int_{-L/2}^{L/2} A(x)\phi(x)dx\right]^2 - I_o \int_{-L/2}^{L/2} A(x)\phi^2(x)dx$$

$$- \psi I_o \int_{-L/2}^{L/2} A(x)\phi(x)xdx - \psi^2 I_o \int_{-L/2}^{L/2} A(x)x^2dx \qquad (49)$$

with $$I_o \equiv \int_{-L/2}^{L/2} A(x)dx$$

We finally are in a position to solve for ψ_{max} which is given by the equation

$$\frac{d\left|f(\psi)\right|^2}{d\psi} = 0 \qquad (50)$$

Our result is

$$\psi_{max} = -\frac{\int_{-L/2}^{L/2} A(x)\phi(x)xdx}{2\int_{-L/2}^{L/2} A(x)\,x^2dx} \qquad (51)$$

and

$$\psi_{max}^2 = \frac{\int_{-L/2}^{L/2} A(x)A^*(x_1)\ \phi(x)\ \phi^*(x_1)\ x x_1 dx dx_1}{4\left[\int_{-L/2}^{L/2} A(x)\ x^2 dx\right]^2} \qquad (52)$$

Taking averages we see that

$\overline{\psi_{max}} = 0$, by virtue of Equation (31), and $\overline{\psi_{max}^2}$ is proportional to the integral of the correlation function since

$$\overline{\phi(x)\ \phi^*(x_1)} = \sigma^2 \int_{-L/2}^{x} \int_{-L/2}^{x_1} e^{-|x' - x''|/\rho}\, dx' dx'' \qquad (53)$$

This integral can be evaluated in a straightforward manner and for the case of N + 1 discrete elements provides the result:

$$\frac{\lambda^2}{\left[\sum_{m=-N/2}^{N/2} A_m\, m^2\right]^2}\ \overline{\psi_{max}^2} = \frac{\rho^2 \sigma_{k_g}^2}{(\alpha/\lambda)^2} \left\{ \sum_{m=-N/2}^{N/2} \sum_{n=-N/2}^{M} A_m A_n \left\{ \left[\left(\frac{nd + L/2}{\rho} \right) + e^{-(nd + L/2)/\rho} - 1 \right] - \frac{1}{2}\left[e^{nd/\rho} - e^{-L/2\rho} \right]\left[e^{-nd/\rho} - e^{-md/\rho} \right] \right\} mn \right.$$

$$\left. - \frac{1}{2} \sum_{m=-N/2}^{N/2} A_m^2 \left[\left(\frac{md + L/2}{\rho} \right) + e^{-(md + L/2)/\rho} - 1 \right] m^2 \right\}$$

With the aid of Equations (47, 48 and 54) we are able to evaluate the mean and variance of the pointing angle error as a function of σ^2 and ρ. Actual numerical results have been done for the 75 element antenna previously described. Results are shown in Figures 11 and 12.

Once again, considering standard X-band waveguide $\left(\frac{2\Delta}{\lambda} \approx 3\text{x}10^{-3}, \sigma\lambda \approx 3\text{x}10^{-2}\right)$ we find that the average pointing error can be expected to be very small. Figure 12 indicates on the order of 10^{-2} degrees with a standard deviation of about 10^{-1} degree.

SECTION IV

SUMMARY AND CONCLUSIONS

This paper has analyzed several factors concerned with operating a slotted waveguide antenna near dominant mode cutoff. The inherent simplicity of this concept for narrow scan application can be seen from the basic scan equations developed in Section II.

The scan equations and the design curve in Figure 5 demonstrate the utility of operating near cutoff in a narrow scan application. Near cutoff we find that suitable steering can be achieved with acceptable bandwidths.

The main concern with operating near cutoff is the sensitivity of the resulting antenna pattern with design tolerances. In particular the sensitivity of guide wavenumber with errors in waveguide dimensions poses an area of concern. This question has been analyzed by considering the effect of a randomly varying guide wavenumber on the antenna pattern.

Theoretical results indicate that it is indeed practical to operate within 1% to 2% of waveguide cutoff without demanding unreasonable design tolerances. It has been shown that errors of a few thousandths of an inch slightly degrade the antenna pattern. A more important effect are the errors in main beam pointing direction introduced by guide wavenumber errors. It is predicted that standard X-band waveguide ($\pm$ .003" tolerance) will produce an r.m.s. pointing error of 0.1°. Increasing waveguide tolerance to $\pm$ .001" reduces this r.m.s. error to about 0.05°.

It should be noted, however, that the r.m.s. pointing angle errors assume complete randomness of the waveguide dimension error (i.e., infinite correlation distance). From Figure 11 we see that the r.m.s. error is reduced significantly as the correlation length decreases; a vanishing correlation length corresponds to a fixed bias error with zero r.m.s. error and a fixed pointing angle error given by Figure 11.

Where the theoretical analysis presented has been applied to guide wavenumber errors the analytical results can be applied to more general error sources. This can be accomplished by determining the mean and variance of guide wavenumber produced by more general random error sources than those considered in this work. It is in this area that more work theoretical and emperical is needed to further examine the feasibility of operating near cutoff.

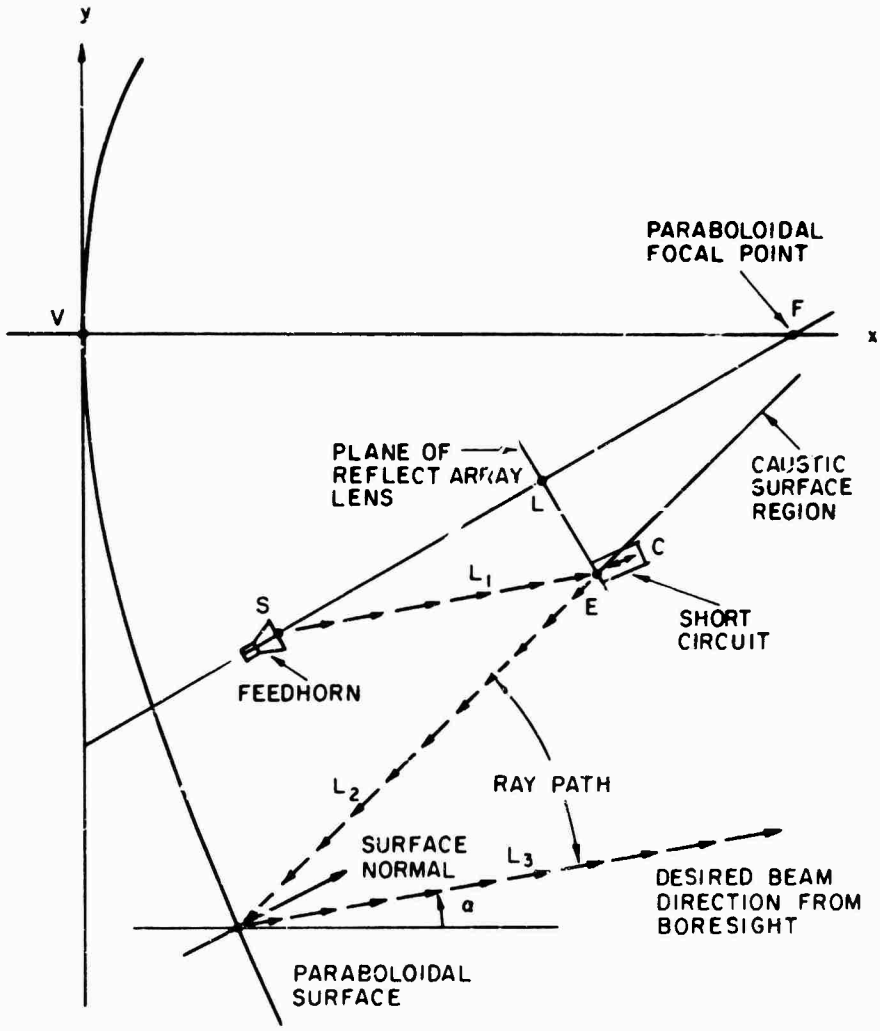

IA-4 272

Figure 1 TPN-19 ANTENNA SYSTEM GEOMETRY

IA-43,274

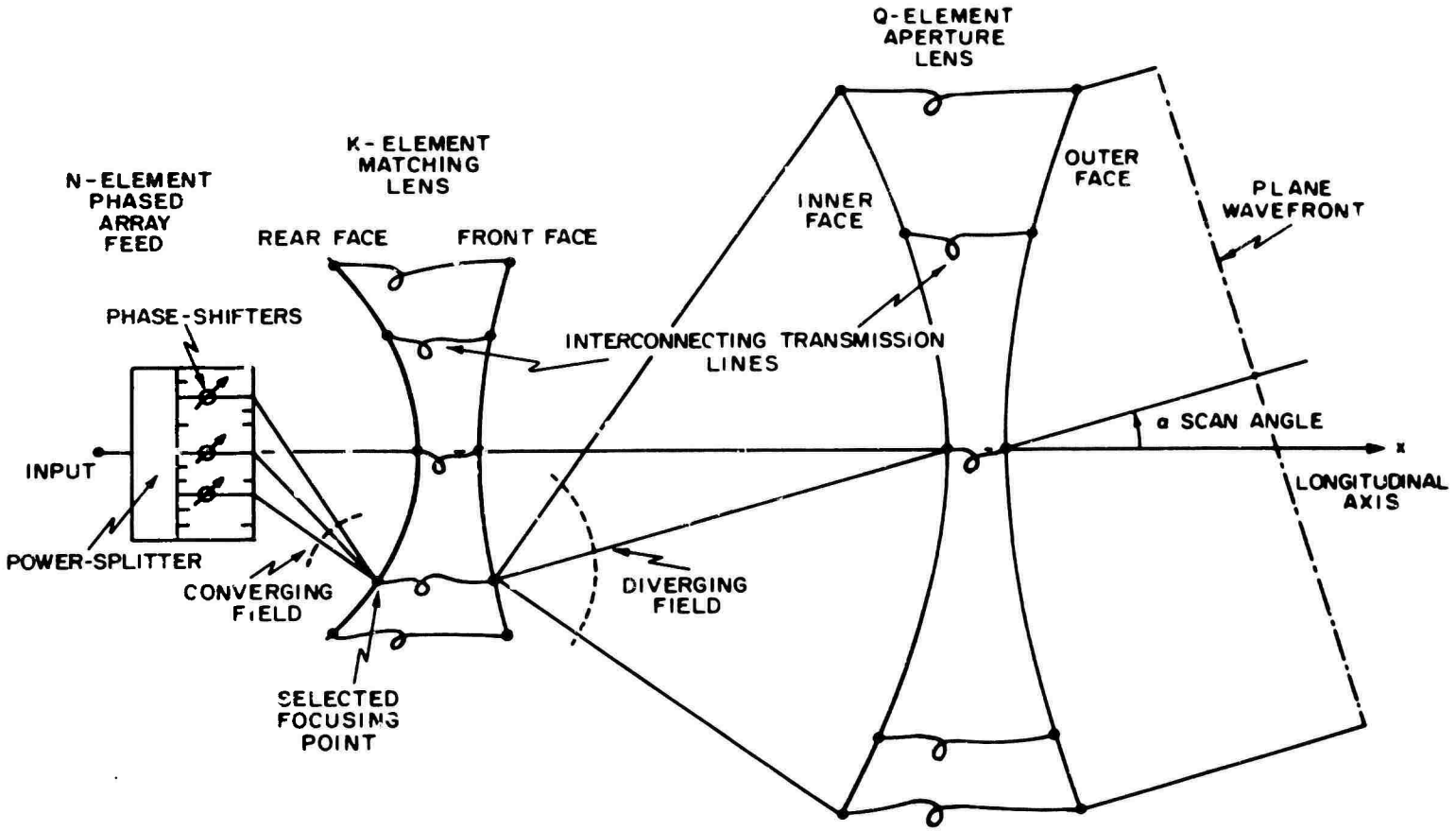

Figure 2 DUAL LENS LIMITED SCAN ANTENNA CONCEPT

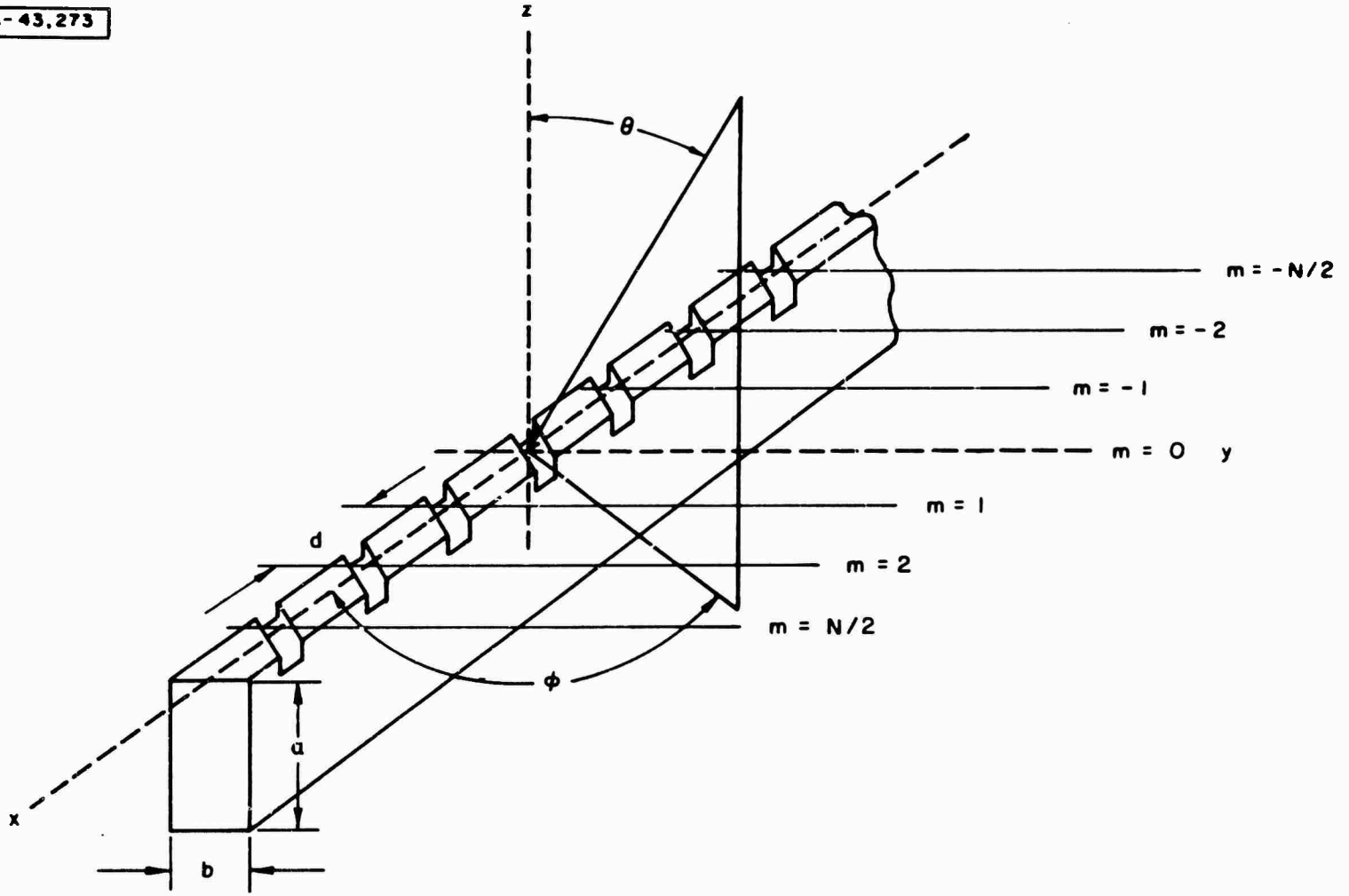

Figure 3 FREQUENCY SCAN SLOTTED WAVEGUIDE CONCEPT

IA-43,275

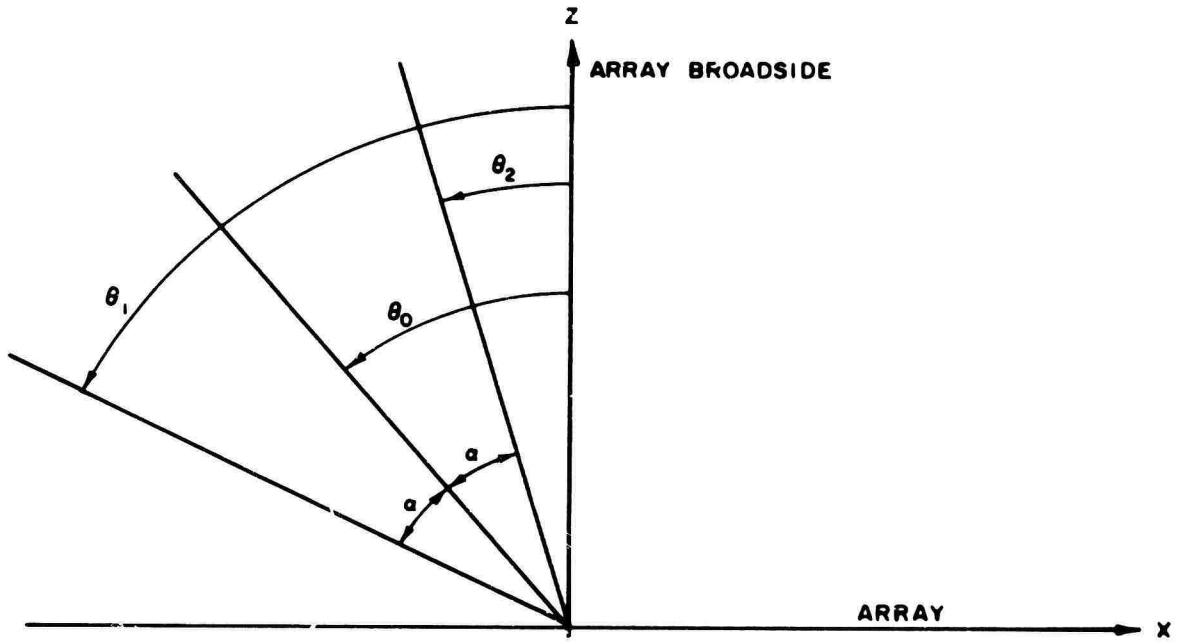

Figure 4 SCAN PARAMETERS

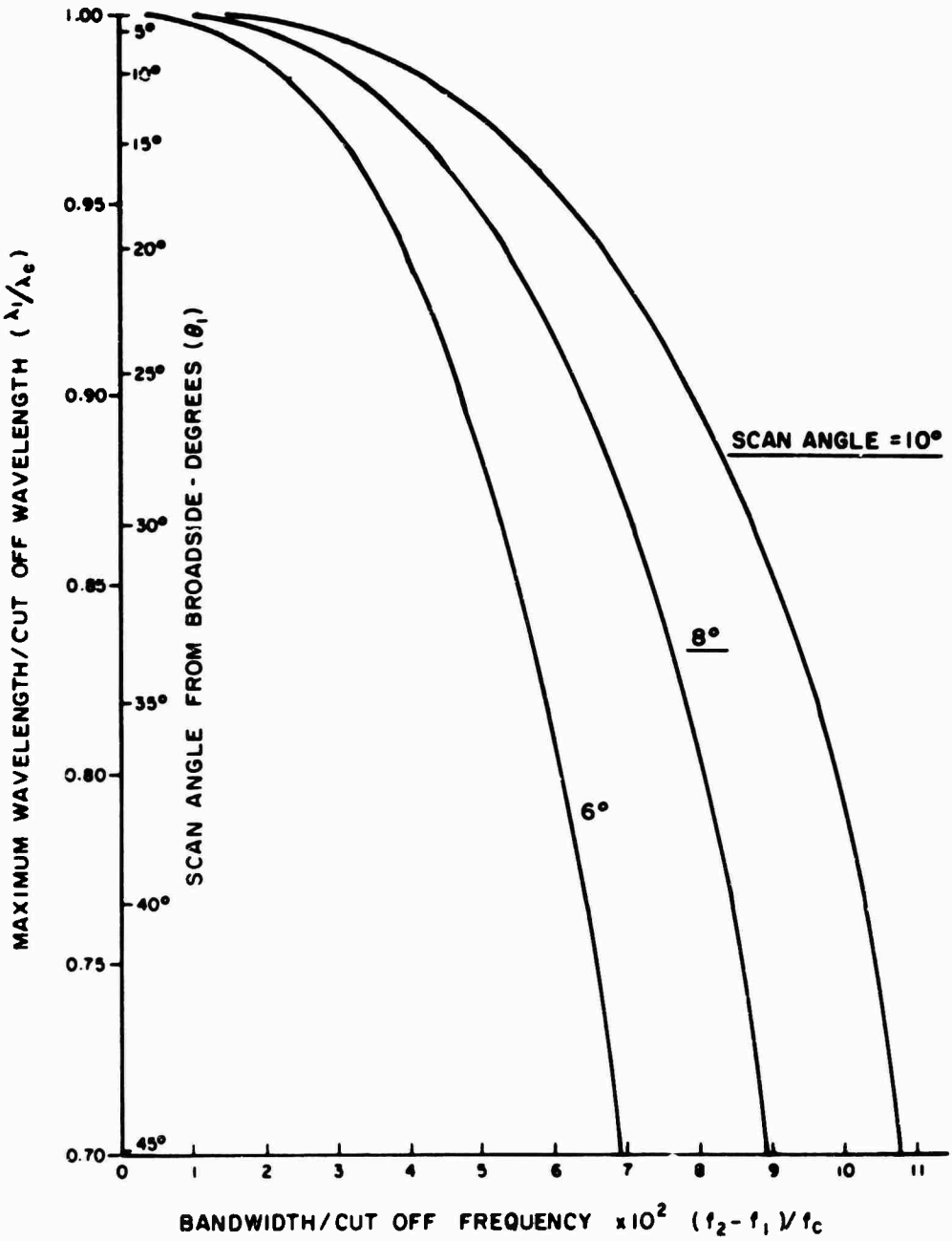

IA-43,276

Figure 5 FREQUENCY SCAN ANTENNA DESIGN CURVE

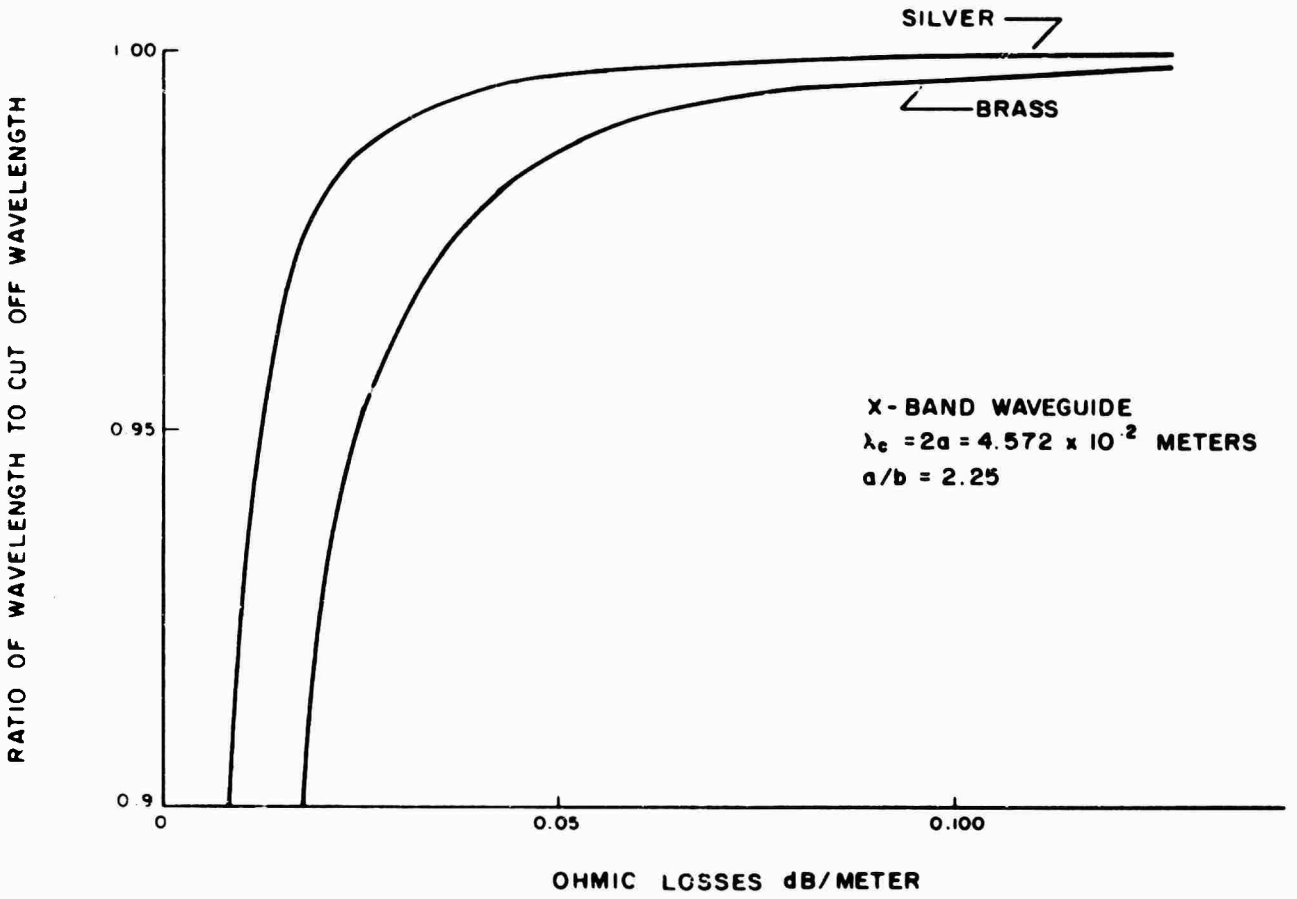

Figure 6 OHMIC LOSSES IN WAVEGUIDE NEAR CUT-OFF

IA-43,277

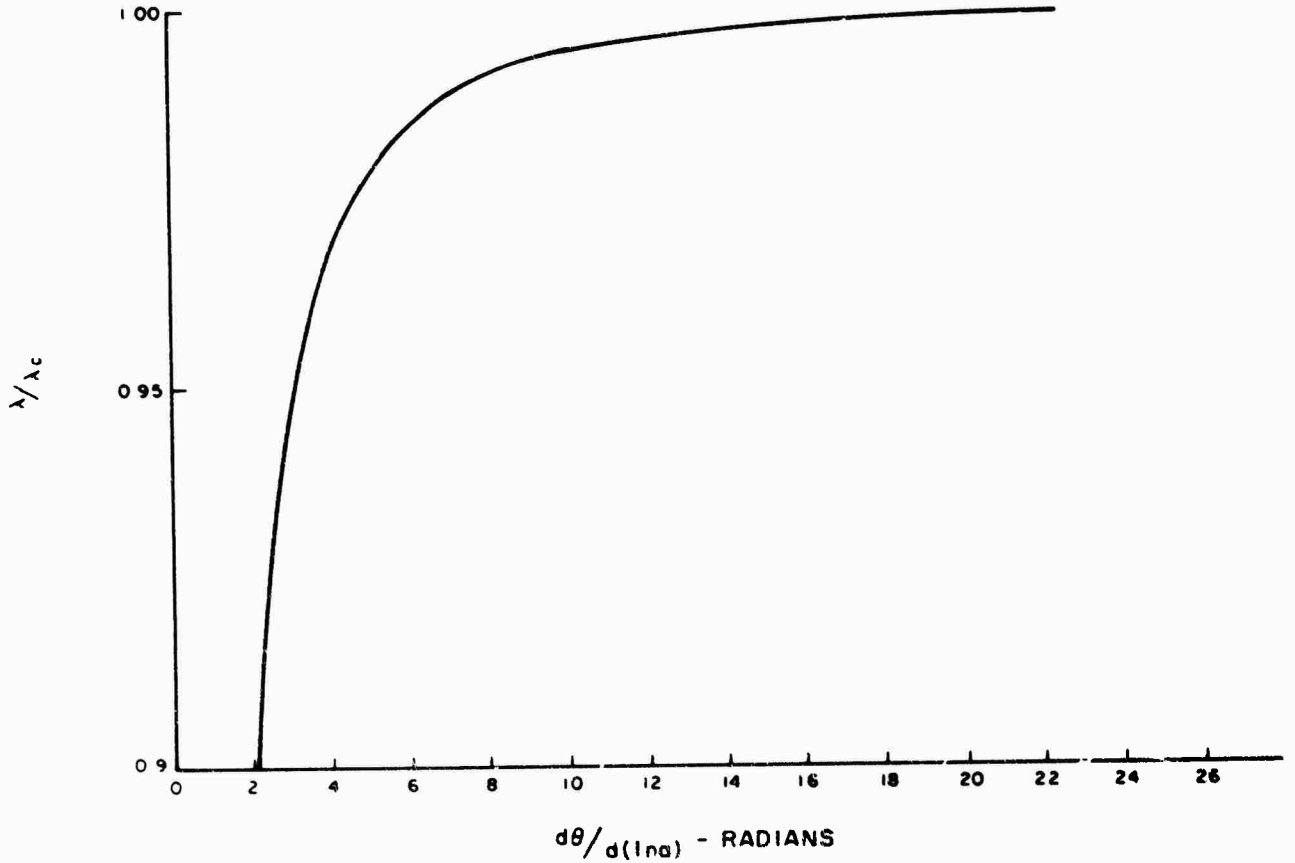

Figure 7 SCAN SENSITIVITY NEAR CUT-OFF

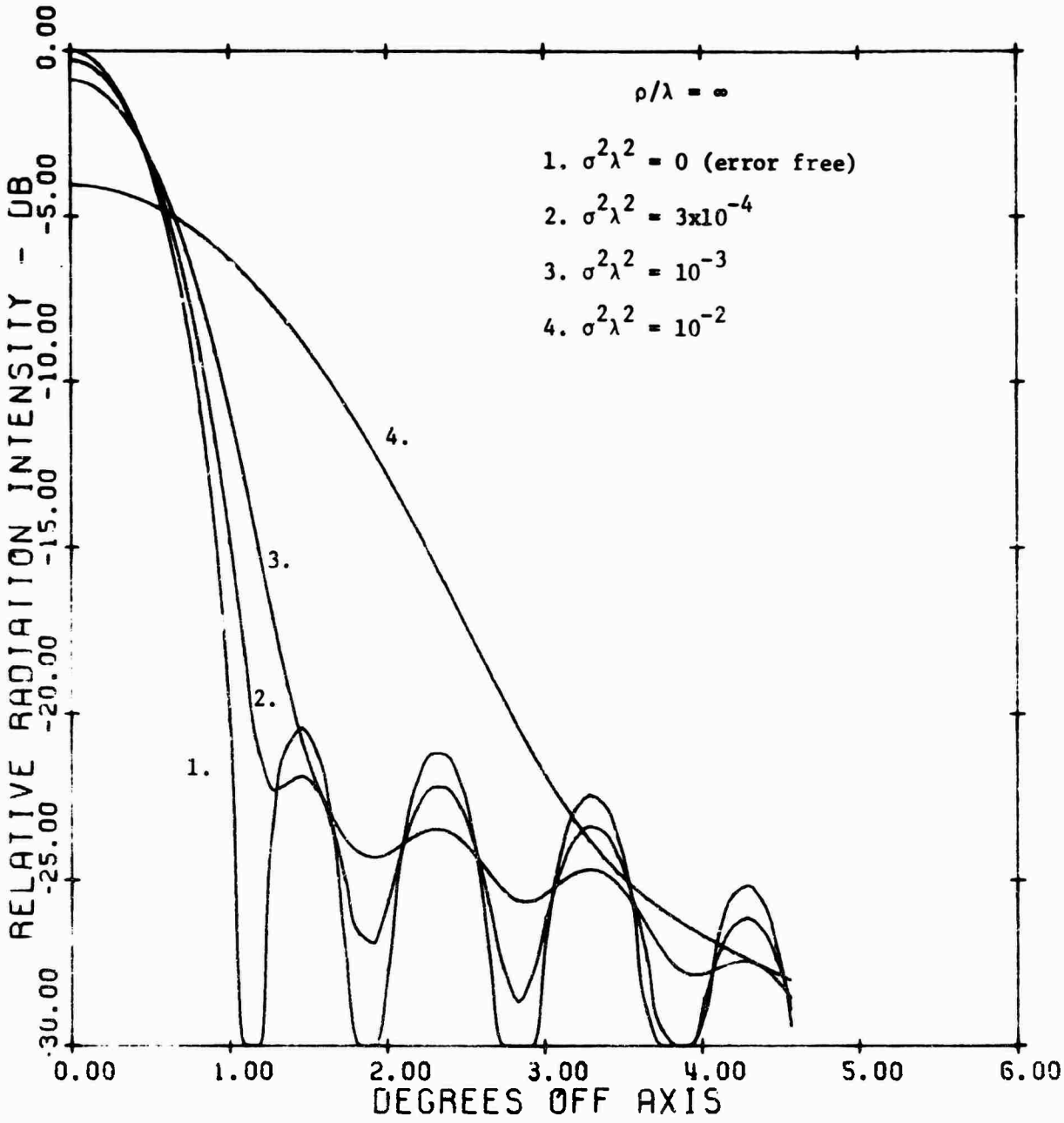

FIGURE 8 AVERAGE RADIATION PATTERNS I

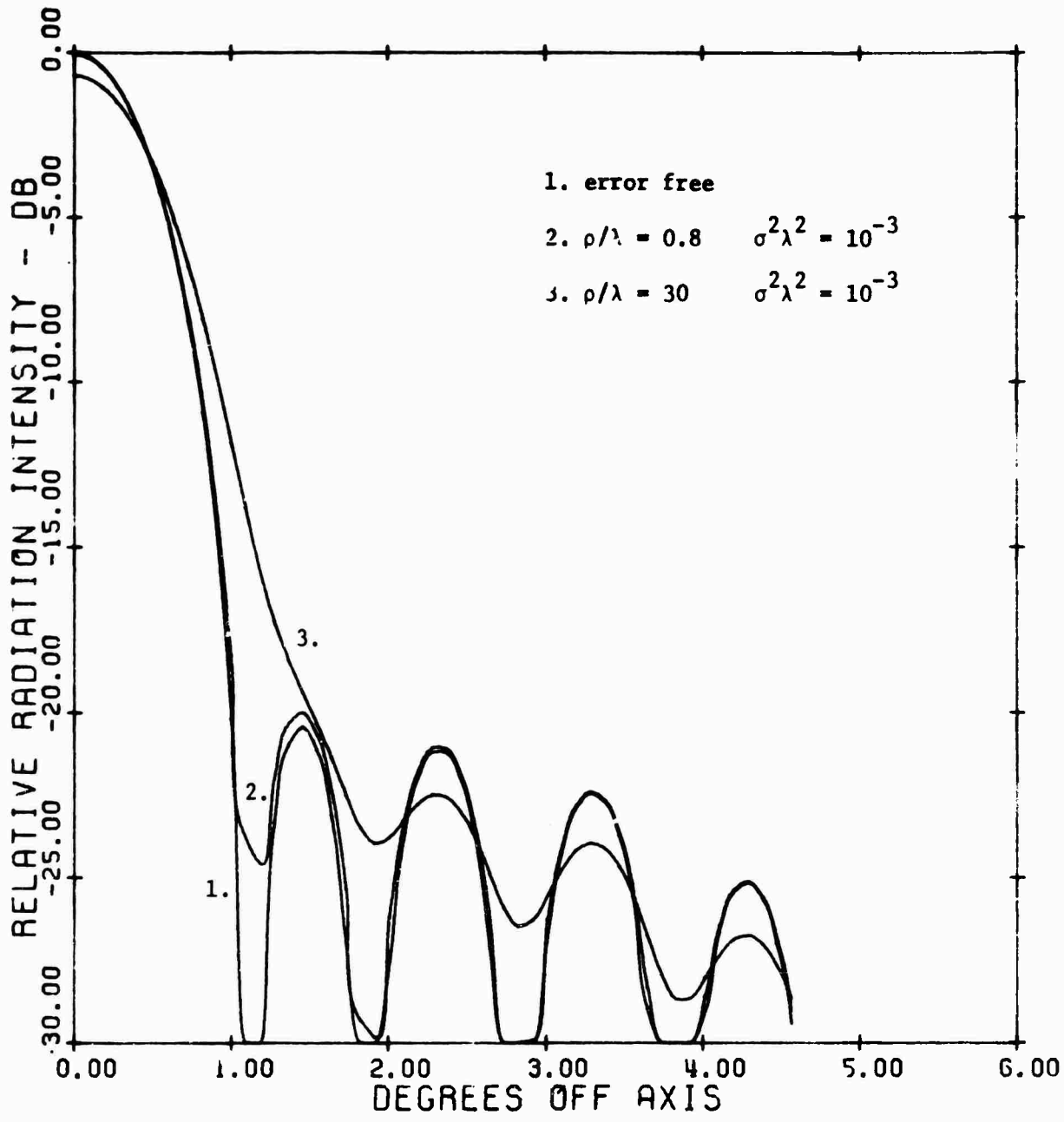

FIGURE 9 AVERAGE RADIATION PATTERNS II

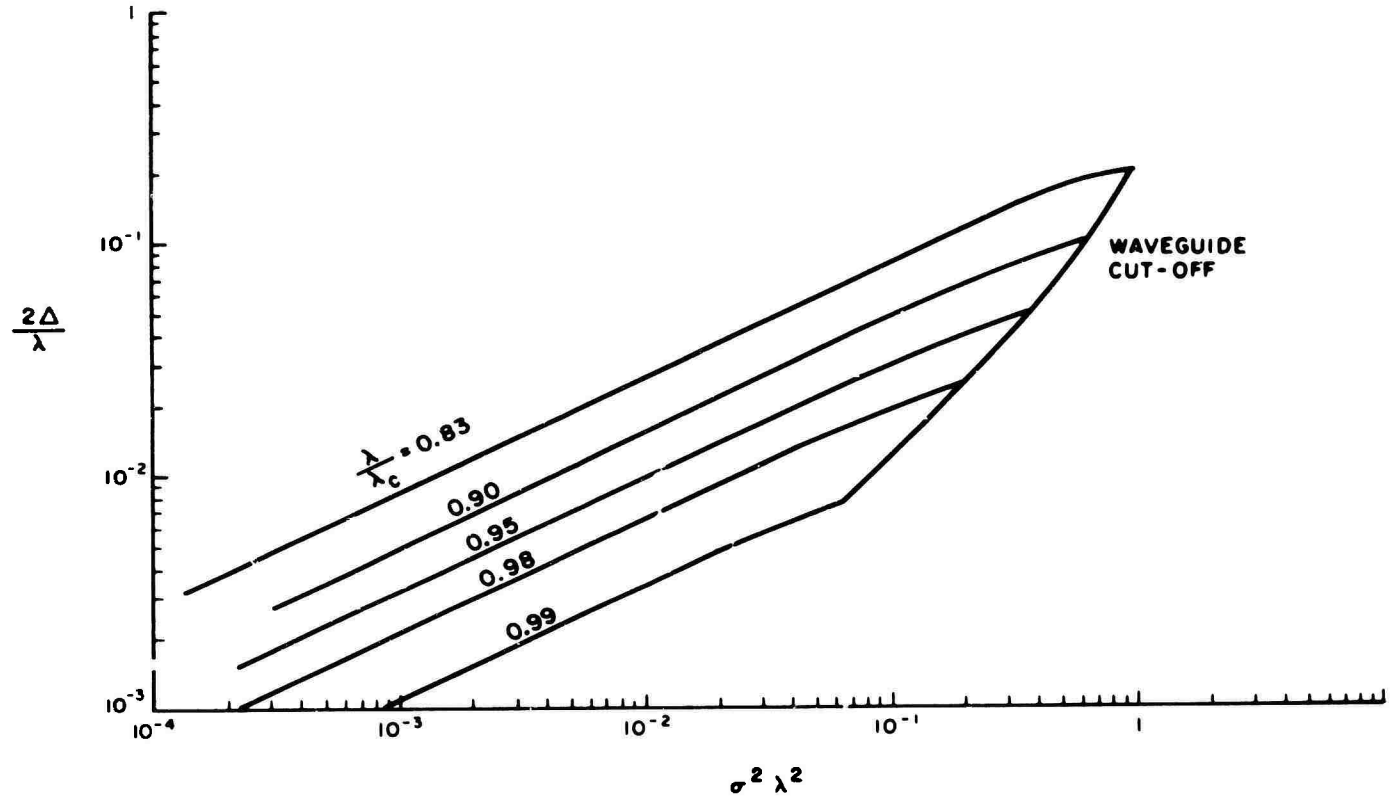

Figure 10 GUIDE WAVE NUMBER VARIANCE

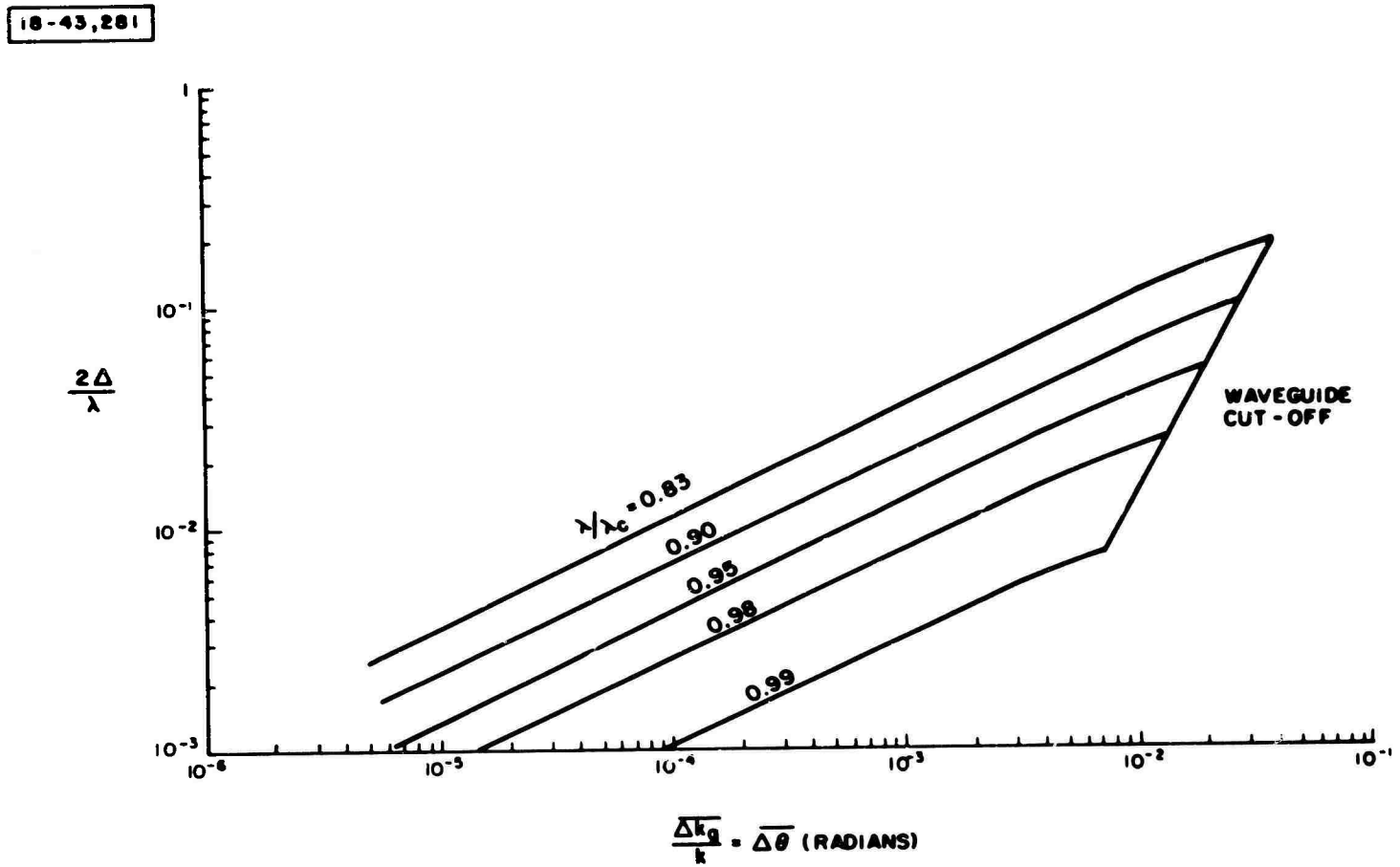

Figure 11 AVERAGE POINTING ANGLE ERROR

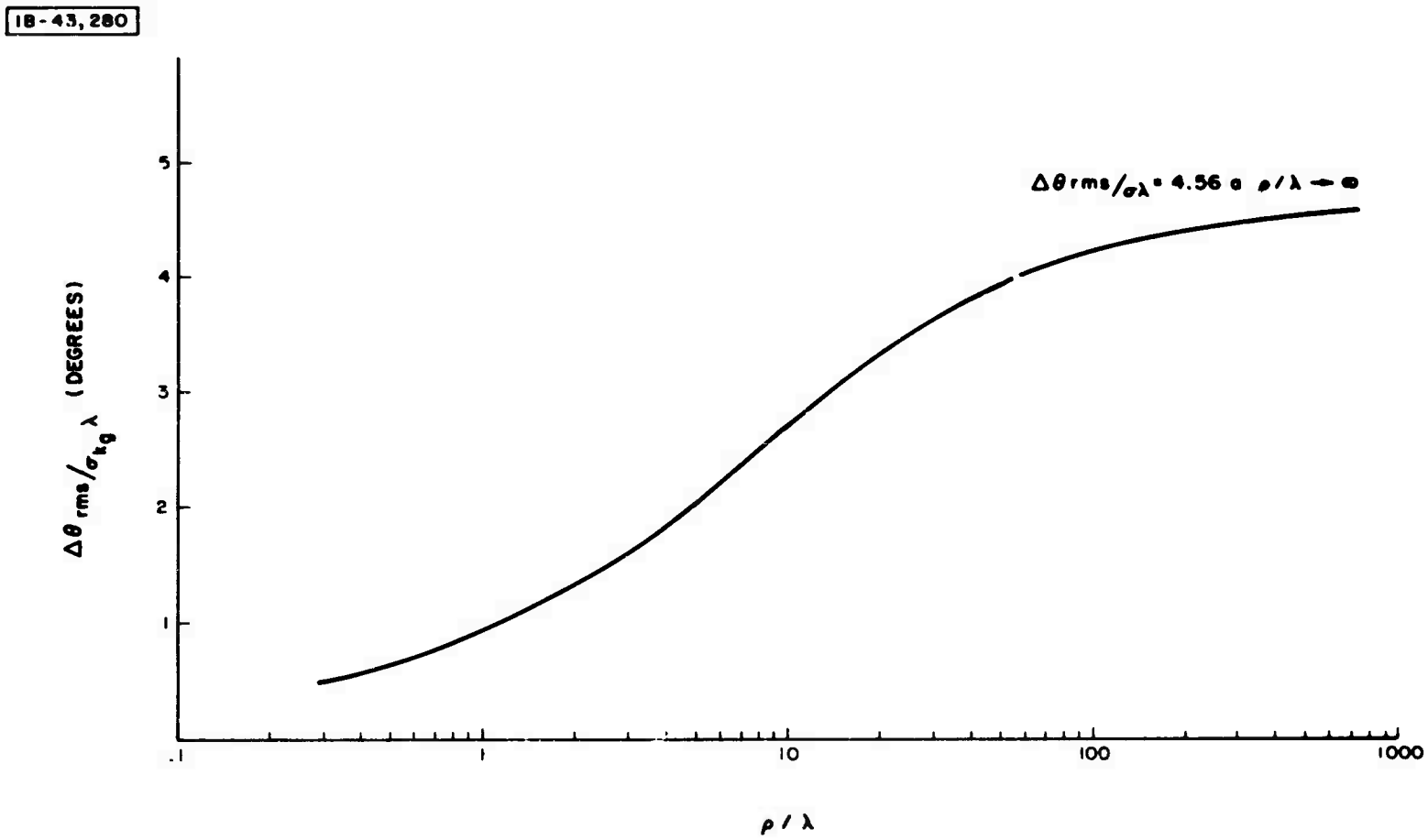

Figure 12 RMS POINTING ANGLE ERROR

REFERENCES

1. AN/TPN-19 Contract End Item Specification CEI No. 321000A, December 1969.

2. A. C. Schell, "Performance of a Reflector-Array Limited Scan Technique" 1973 PGAP Symposium Record Boulder, Colorado, August 1973.

3. R. J. Mailloux and G. R. Forbes, "An Experimental Array Program for Limited Scan Studies", 1973 PGAP Symposium Record Boulder, Colorado, August 1973.

4. R. J. Mailloux, "Array Techniques for Limited Scan Application", AFCRL-72-0421, July 1972.

5. C. H. Tang and C. F. Winter, "Study of Use of Phased Array to Achieve Pencil Beam Over Limited Sector Scan", AFCRL-TR-73-0482, July 1973.

6. S. Ramo and J. R. Whinnery, "Fields and Waves in Modern Radio", Wiley and Sons, N.Y. 1953, page 368.

7. Ibid, page 240.

8. Y. S. Shifrin, "Statistical Antenna Theory", The Golem Press, Boulder, Colorado, 1971.

9. S. Wilkes, "Mathematical Statistics", Wiley and Sons, N.Y., pages 257-258.

10. R. J. Spellmire, "Tables of Taylor Aperture Distributions", Hughes Aircraft JM #581, October 1958.